LA-UR- 09-07755

Approved for public release; distribution is unlimited.

Title:	HOT SPOT-DERIVED SHOCK INITIATION PHENOMENA IN HETEROGENEOUS NITROMETHANE
Author(s):	D. M. Dattelbaum, S. A. Sheffield, D. B. Stahl, A. M. Dattelbaum
Intended for:	2009 Joint Army-Navy-NASA-Air Force (JANNAF) meeting, La Jolla, CA, Dec. 7-11, 2009

Los Alamos
NATIONAL LABORATORY
EST. 1943

Form 836 (7/06)

HOT SPOT-DERIVED SHOCK INITIATION PHENOMENA IN HETEROGENEOUS NITROMETHANE

D. M. Dattelbaum, S. A. Sheffield, D. B. Stahl, A. M. Dattelbaum
Shock and Detonation Physics, Los Alamos National Laboratory
Los Alamos, NM 87545

ABSTRACT

The addition of solid silica particles to gelled nitromethane offers a tractable model system for interrogating the role of impedance mismatches as one type of hot spot "seed" on the initiation behaviors of explosive formulations. Gas gun-driven plate impact experiments are used to produce well-defined shock inputs into nitromethane-silica mixtures containing size-selected silica beads at 6 wt%. The Pop-plots or relationships between shock input pressure and run-distance (or time)-to-detonation for mixtures containing small (1-4 μm) and large (40 μm) beads are presented. Overall, the addition of beads was found to influence the shock sensitivity of the mixtures, with the smaller beads being more sensitizing than the larger beads, lowering the shock initiation threshold for the same run distance to detonation compared with neat nitromethane. In addition, the use of embedded electromagnetic gauges provides detailed information pertaining to the mechanism of the build-up to detonation and associated reactive flow. Of note, an initiation mechanism characteristic of homogeneous liquid explosives, such as nitromethane, was observed in the nitromethane-40 μm diameter silica samples at high shock input pressures, indicating that the influence of hot spots on the initiation process was minimal under these conditions.

INTRODUCTION

The generation of "hot spots," or localized regions of high temperature and pressure, defines the shock initiation sensitivity and initiation mechanisms of most solid high explosives, whether conventional, insensitive, or non-ideal. The *potential* origins of hot spots within a material include dynamic pore collapse, friction or shear along sliding interfaces, wave reflections from *in-situ* impedance mismatches, and others.[1-3] However, despite many decades of research into the physics of high explosives, at present we only have a very basic understanding of the broad mechanisms underlying shock-induced hot spot generation, subsequent hot spot ignition, and the confluence of multiple hot spots leading to reactive wave build-up and detonation.

The concept of hot spots as it pertains to explosives initiation is not new.[1-3] There have been numerous estimates of the "critical" hot spot size and temperature leading to initiation for various explosive formulations. Estimates by Bowden and Yoffe, as early as the 1950s, placed values on the critical hot spot size at 0.1-10 micron, temperature >700K, and duration of 10^{-5}-10^{-3} sec.[1] A number of studies have since aimed to deconvolute the influence of microstructural features on explosives sensitivity, revealing that hot spot formation and growth is a complicated time- and length scale-, material-dependent process. Motivated by the often trial-and-error process of developing new explosive formulations, investigations linking grain size to either the critical diameter or run-distance-to-detonation have been performed for formulations containing such explosives as RDX, PETN, and TNT.[8-11] Further, porosity has been examined as a different type of hot spot "seed", either through the study of pressed explosives at varying initial densities (as percentages of the theoretical maximum density), or by the introduction of glass microballoons into liquid, slurry, and solid explosives.[12-15] Complicating the analysis of these experimental studies is that every explosive has its own innate chemical reactivity, and the outcome is intertwined with the characteristics of the stimulus (shock strength, shock pulse

duration, etc.), and the number of experimental tests are often sparse due to the cost of both the formulations and testing.

From a theoretical standpoint, hot spot concepts form the basis of the ignition and growth model[16], where the model, representing separate hot spot ignition and growth phases, is calibrated to experimental shock initiation data. More recently, it has been suggested that the incorporation of geometric term(s) to reactive burn models, representative of the real microstructures that give rise to hot spots, may improve our ability to predict the shock sensitivity of explosive formulations.[19, 35, 36] Bouton *et al.,* for example, have shown that both the critical diameter and run-distance-to-detonation at a fixed input shock pressure, can be correlated with the specific surface area of either the explosive grains, or inert additives that are suspected to give rise to hot spots.[19]

Here, we report the results of an experimental study to further elucidate critical features of hot spots and their relation to shock initiation mechanisms and thresholds, using a well-defined model system that allows for tuning of the hot spot number density formed during shock compression. Solid particles, of relevant sizes in the micron-range, have been intentionally introduced into the otherwise-homogeneous liquid explosive nitromethane (NM). The tunability of the mixture provides a system that is useful for interrogating the influence of shock impedance mismatches as one type of hot spot "seed". In addition to measurements of the run-distance-to-detonation as a function of shock input pressures, the application of embedded electromagnetic gauges allows for *in-situ* measurement of the reactive flow, giving insights into the nature of the build-up to detonation. Two series of experiments have been performed for gelled nitromethane loaded with 6 wt% solid silica beads with small (~1-4 μm) and large (40 μm) diameters. By keeping the weight percentage constant, the interparticle distance is also varied between the two mixtures.

EXPERIMENTAL

Nitromethane (NM, CH_3NO_2) was purchased from Sigma-Aldrich (99+%) and used without further purification, with a freshly-opened sample used for each experiment. Guar gum (General Mills 512 Guar, a cyanoethylether of a galactomannan gum), was the same as that used by Engelke.[4,5] Solid silica particles of 1-4 and 40 μm diameters were obtained from Particle Information Services. Particle sizes were confirmed using both optical and scanning electron microscopies.

Samples for plate-impact experiments were prepared by weighing out appropriate quantities of NM, Guar, and silica to prepare mixtures consisting of 92.25 wt% NM, 1.75 wt% Guar, and 6 wt% silica. The silica particles were added to the NM in a high-walled beaker, followed by slow addition of Guar with continuous stirring to gel the mixture. The resulting white, viscous mixture was then pipetted into a LANL-designed liquid target cell, shown schematically in Figure 1 (left).[6] A photograph of a partially assembled target cell is shown in Figure 1 (right).

Plate-impact experiments were performed using the LANL 50 mm-bore two-stage light gas gun described previously.[7] Kel-F 81 (polychlorotrifluoroethylene) impactors saboted in Lexan projectiles were launched at velocities up to ~2.9 km/s at instrumented targets containing the NM mixtures. Embedded electromagnetic gauges, described previously, [6-8] provided *in-situ* shock wave profiles at ten Lagrangian positions, allowing for determination of both the initial, unreacted shocked state (Hugoniot locus) and run-distance (or time)-to-detonation. A photograph of an electromagnetic gauge package is shown in Figure 2. The horizontal elements in the center of the gauge package give the shock wave profiles at nine different positions in the sample, and are used in combination with a single-element "stirrup gauge" at the PMMA-NM input interface (as can be seen in Figure 1, right). The finely-patterned gauge elements on either side and at the bottom center of the package are referred to as the "shock trackers," which give high precision measurements of wave arrival at each element, redundantly determining the shock and/or detonation wave velocities in the experiments.

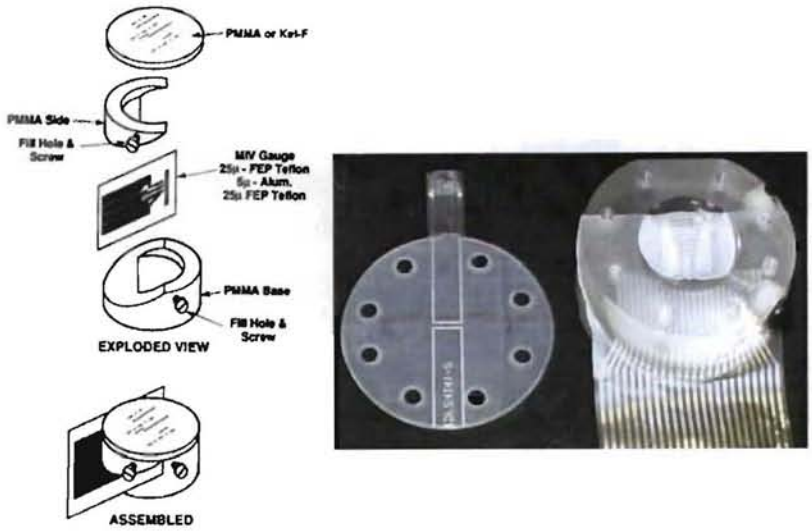

Figure 1. (left) Expanded view of LANL liquid target cell designed for making embedded gauge measurements in liquid explosives under gas gun-driven shock compression, and (right) Photograph of a liquid cell with the top off, showing the embedded gauge at a 30° angle.

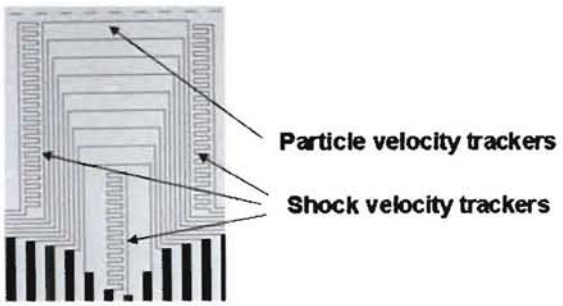

Figure 2. Photograph of embedded gauge membrane showing the patterned Al gauge elements.

RESULTS AND DISCUSSION

Neat NM is one of the most well-characterized liquid explosives in terms of its equation of state (EOS), initiation and detonation properties.[4-6, 24-33] NM has a steady detonation velocity of 6.23 mm/μs, estimated Chapman-Jouguet (CJ) pressure P_{CJ} = 12.5 GPa, and failure diameter of 16.2 mm in pyrex glass.[24] The detonation characteristics of NM have been previously shown to be susceptible to both chemical and physical sensitization as shown by either reduction in critical (failure) diameters, or lowering of shock initiation thresholds.[4-6,17-19] Recently, we reported detailed measurements of the chemical reaction zone of NM.[24] The reaction zone has a predicted von Neumann spike particle velocity of 2.7 mm/μs, and sonic/CJ state of 1.8 mm/μs. The temporal decay of the particle velocity through the reaction zone is marked by a fast and slow component. Decay of the fast component occurs within the first ~10 ns behind the front, followed by a slower decrease in particle velocity over ~ 100 ns. Based on the predicted CJ condition from the unreacted and product equations-of-state for NM, the overall reaction zone length was estimated to be ~ 100-150 ns, or 600 to 900 microns in width.

A means of judging the shock sensitivity of explosives is through the development of "Pop-plots" or the relationship between the shock input pressure and the run-distance (or overtake

time) to detonation.[7] The Pop-plot for neat NM has been well-established by numerous sources, and the data is collectively shown in Figure 3.[28-30] Compared with the conventional plastic-bonded explosive PBX 9501, a mixture of 95 wt% HMX with 5% Estane/nitroplasticizer binder,[37] NM is less sensitive to initiation by shock compression, requiring almost twice the shock input pressure for the same run distance. The shallow slope of the data in the Pop-plot also reveals the high dependence of the initiation behavior on temperature. A small change in the shock input pressure, and therefore small change in temperature, results in a large difference in the run-distance-to-detonation, as seen in Figure 3.

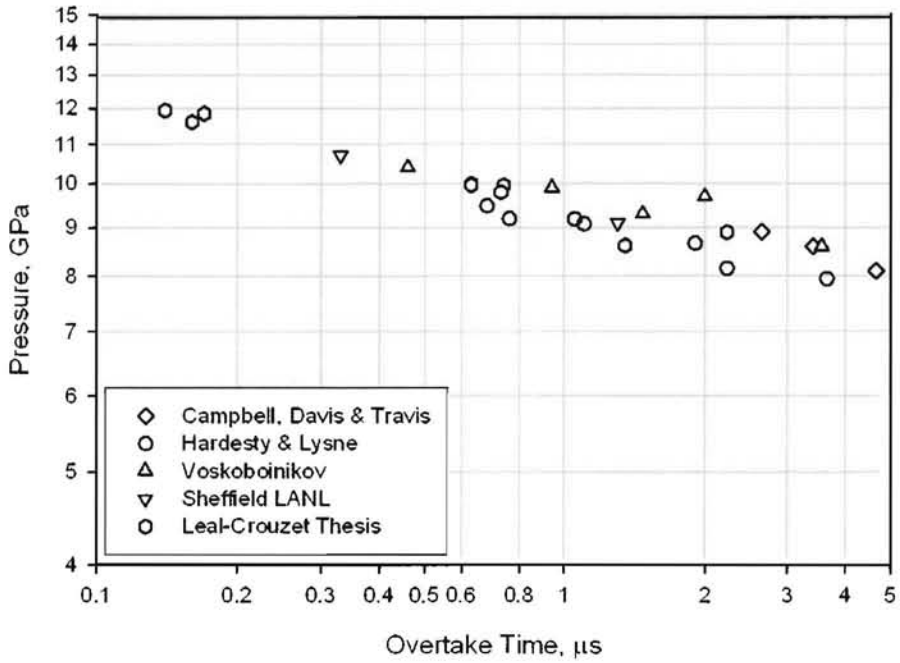

Figure 3. Shock input pressure vs. detonation overtake time (Pop-plot) for neat nitromethane.

Engelke has previously shown that the addition of rough (uncontrolled particle morphologies, 5-75 mm diameters) silica at 6 wt% to NM, gelled with guar gum, results in a dramatic reduction in the critical diameter compared to neat NM.[4] In addition, the failure behavior was found to be more similar to that of heterogeneous explosive formulations, such as plastic bonded explosives, in which a large velocity deficit could be sustained prior to failure (e.g. the detonation would propagate in smaller charge radii but at lower velocities compared to the large diameter steady velocity). For 92.75/6/1.25 wt% NM/silica/guar, the failure diameter was reduced to 9.6 mm compared with 16.2 mm for neat NM. To isolate the influence of particle size, Engelke further performed a series of failure experiments, varying the number density and diameter of controlled silica beads in gelled NM. He found that reductions in the critical diameter were most profound for small (1-4 mm) silica beads, and that there is a correlation between the reduction in critical diameter and mean interparticle separation.[5] Similarly, Bouton has suggested that critical diameter can be correlated to specific surface area of added particles for a wide variety of explosive formulations.[19] The reduction of critical diameter is posited to be tied to the influence of hot spots affecting the chemical reaction zone length, and enabling detonation propagation in smaller charge radii. It has been suggested that the critical diameter is related to the chemical reaction zone length by:

$$D_R = D_\infty (1 - \frac{A}{R})$$

where D_R is the steady detonation velocity of a two-dimensional detonation traveling in a cylindrical charge with radius R, D_∞ is the infinite diameter steady detonation velocity, and A is a fitting parameter, which *may* be related to the steady one-dimensional chemical reaction zone length.[31-33] Engelke *et al.* found that the relationship between critical diameter and reaction zone length was not linear for samples of nitromethane containing the chemically-sensitizing diethylenetriamine at varying concentrations, albeit there did appear to be a relationship between the quantities.[31-32] The failure characteristics of nitromethane-silica mixtures established by Engelke provide a foundation for the work presented here. To gain an understanding of the influence of hot spot number density and type on *initiation* characteristics, some of the same mixtures studied by Engelke have been investigated here using well-defined shock wave inputs to initiate the NM-silica mixtures.

Gas gun-driven shock initiation experiments have been performed on gelled nitromethane samples containing solid silica beads at 6 wt%. The diameters of the silica particles have been chosen to be 1-4 μm or 40 μm, and are the same materials used by Engelke.[ref] From each experiment, numerous details about the shock-to-detonation transition are gleaned, including measurements of the initial unreacted shocked state or Hugoniot locus, shock and particle velocities associated with the initial shock, reactive and detonation waves, and run-distance or time-to-detonation as a function of shock input pressure for population of the Pop-plot. To ensure that gellation of the nitromethane did not affect its shock initiation properties, a single experiment was performed on gelled nitromethane (1.75 wt% guar) with the Pop-plot point falling within the data for neat liquid NM.

The results of two series of shock initiation experiments are summarized in Table 1. Variation of the projectile velocity using the same projectile-impactor combination results in variation in the initial shock pressure imparted to the target cell, and thus the nitromethane-silica mixtures. The input shock pressure was determined by the measurement of the initial shock and particle velocities and application of the Rankine-Hugoniot conservation equations to calculate pressure (initial density = 1.15 g/cm^3) or by impedance matching methods using the measured initial particle velocity and Kel-F 81 Hugoniot-based equation of state. The time to detonation was determined as the time from the initial shock at the target front-NM interface to the observation of leading detonation wave at one of the nine embedded particle velocity gauges (or Lagrangian positions). Comments pertaining to the initiation mechanism, as described below, are also listed in the Table.

TABLE 1. Summary of shock initiation experiments on heterogeneous NM with controlled silica particle diameters. P_{in} is the input shock pressure in GPa, t is the shock-to-detonation run time in microseconds.

Shot #	Projectile velocity (km/s)	Particle loading/size	P_{in} (GPa)	Time-to-detonation (μs)	Comments
2S-312	2.045	6 wt% 40 μm silica	5.8	>3.5	Did not turn over
2S-314	2.308	6 wt% 40 μm silica	7.1	2.26	Mixed mechanism
2S-317	2.721	6 wt% 40 μm silica	9.5	1.15	Homogeneous-like
2S-356	2.904	6 wt% 40 μm silica	10.7	0.65	Homogeneous-like
2S-357	2.909	6 wt% 40 μm silica	10.5	0.62	Homogeneous-like
2S-358	2.485	6 wt% 40 μm silica	7.8	1.75	Mixed mechanism
2S-319	2.669	6 wt% 1-4 μm silica	9.3	~0.38	Early turn-over
2S-359	2.235	6 wt% 1-4 μm silica	7.0	1.66	Growth in and behind front
2S-361	2.468	6 wt% 1-4 μm silica	8.5	0.96	Growth in and behind front
2S-397		6 wt% 1-4 μm silica			
2S-					

The Pop-plot points derived from the shock initiation experiments on the two mixtures are shown in Figure 4 overlaid with the data for neat NM. It should be noted that the initiation mechanism is not necessarily the same for either the type of mixture or the input pressure, and the overall turnover time, despite the differences, is used to populate the Pop-plots. As seen in the figure, the addition of silica beads at 6 wt% has a measurable effect on the shock sensitivity. The mixtures of 40 μm silica in NM show non-linear behavior, with a shallow slope at high pressure paralleling the neat NM data, evolving into a steeper slope at lower shock input pressures. The lowest pressure point for this figure, from shot 2S-312, did not turnover during the 1-dimensional time of the experiment, and is thus a lower limit for turnover time. The mixture of 6 wt% 1-4 μm silica in NM shows that the smaller particles are more universally sensitizing, as shown by a decrease in the shock initiation pressure for the same run distance/time compared with neat NM over a large range of shock input pressures. Furthermore, there may be evidence that at low shock input pressures, the data for this mixture begins to deviate even more from neat NM with the initiation threshold for the NM-silica mixture being lower by up to 2 GPa over the measured pressure regime. The slope of the data for this mixture appears to nearly-parallel the Pop-plot for neat NM to ~ 7.8 GPa, or to a run distance near 1.5 μs before appearing to turn down in this plane.

Incorporation of the silica beads into the gelled nitromethane results in hot spots through the interaction of the incident shock with the higher impedance (the shock impedance $Z = c_0 \times \rho$, or the bulk sound velocity times the initial density) particles (e.g. impedance mismatches). Non-reactive simulations of the hydrodynamic flow in a nitromethane sample containing 20 μm silica beads shocked to 10 GPa indicate that the mechanism for hot spot formation is a combination of adjacent nearly-head-on wave collisions occurring between the beads, as well as Mach reflections at the bead-NM interface.[35] Shock reflections normal to the NM-bead interface were not found to appreciably raise the temperature of the nitromethane behind the front.

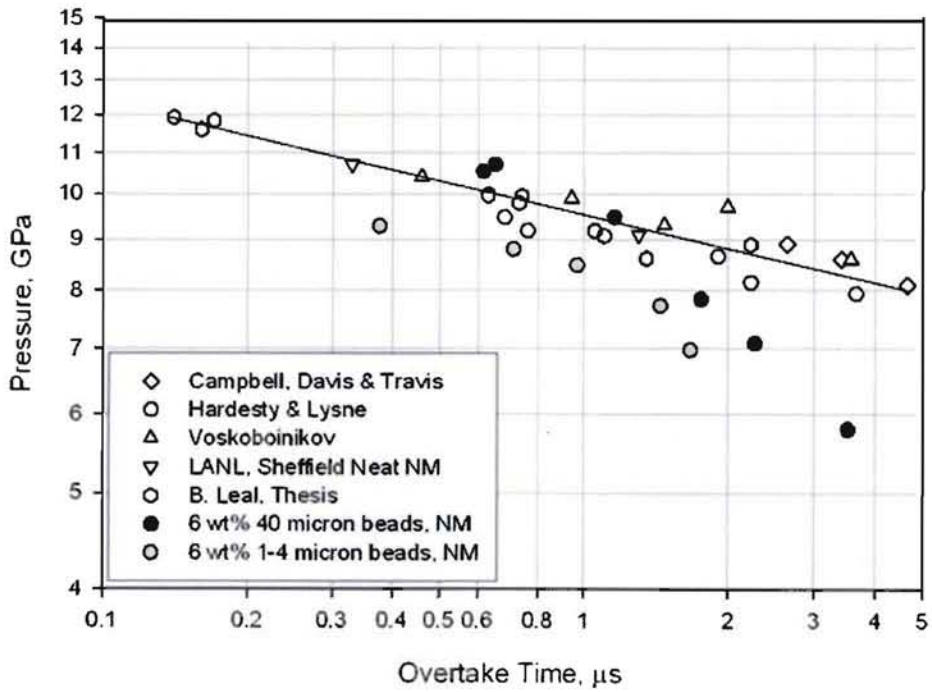

Figure 4. Shock input pressure vs. overtake time to detonation (Pop-plot) for neat and heterogeneous NM containing 40 mm silica. See text for references.

The Pop-plot data are in general agreement with Engelke's findings of the dependence of critical diameter on bead addition. No or little reduction in the critical diameter was observed for the large 40 μm diameter beads at the same weight percentage (likewise for even larger 100 μm

particles). However, a measurable reduction in the critical diameter was observed for mixtures containing the smaller 1-4 μm beads, indicating increased "sensitivity" under failure criteria. Varying the distance between the smaller beads, achieved by variation of the weight percentage, further influenced the decrement in the critical diameter (d_c), with d_c decreasing even further as the interparticle bead separation was reduced. In the Pop-plots above, the large particle samples deviated from neat NM only at shock input lower pressures. By contrast, the samples with the smaller particles showed an overall lowered shock initiation threshold.

The use of embedded electromagnetic gauges allows for *in-situ* measurements of the shock and detonation wave profiles, and offers unprecedented insight into not only the shock-to-detonation run distance, but also the initiation mechanisms of explosives. It is well known that liquid, or homogeneous, explosives exhibit different initiation behaviors compared with solid, multi-phase explosives. The initiation mechanism of neat nitromethane, like other homogeneous liquid explosives, is characterized by thermal explosion that occurs behind the incident shock front after an induction time, and resultant growth of a superdetonation wave traveling in the shock compressed material behind the shock front.[25-27] The superdetonation wave has been observed to travel at high velocities, exceeding 10 km/s, and eventually overtakes the initial shock, leading to an overdriven detonation that settles down to a steady detonation with distance (x) or time (t). This process for homogeneous liquid explosives is shown schematically in the time-distance diagram in Figure 5. The thermal explosion occurs at some time/distance from the shocked boundary after an induction period τ_{ind}, and the reactive wave or superdetonation builds from the thermal explosion over a measurable distance. Eventually, the superdetonation overtakes the initial shock front, as shown by the intersection point in Figure 5.

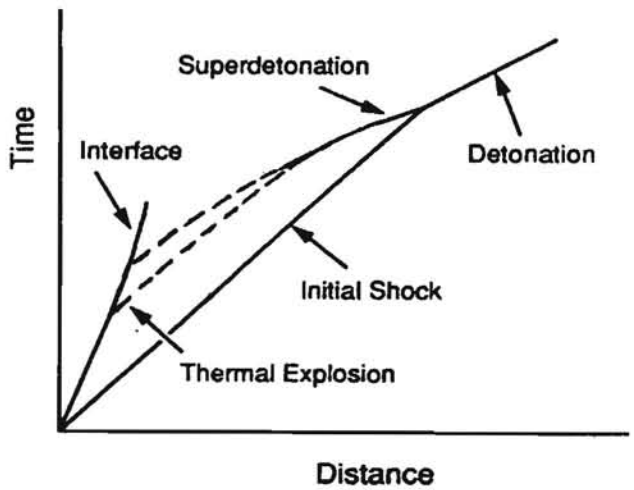

Figure 5. Time-distance (t-x) diagram illustrating the initiation process for homogeneous explosives such as liquid nitromethane.

"Heterogeneous" or multi-phase explosives, such as plastic bonded explosives, by contrast, typically show reactive growth in or near (in time/distance) the shock front, with gradual, continuous reactive growth eventually leading to detonation, see for example reference 37. The specific features of the reactive flow for heterogeneous explosives are dictated by the explosive formulation, e.g. type of energetic crystals, porosity, and related features of the microstructure.

Figure 6 shows the wave profiles associated with the shock-to-detonation transition for shot 2S-361, 92.25/6.0/1.75 wt% NM/1-4 μm silica/Guar, with an initial shock input pressure of 8.5 GPa. From the figure, the reactive flow associated with the build-up to detonation is marked by growth in or near the front, as well as growth temporally and spatially behind the shock front. The particle velocity growth associated with the reactive build-up is continuous, similar to what is

observed for heterogeneous explosives. In fact, remarkably-similar wave profiles have been observed for the shock-to-detonation transition for PBX 9501.[37]

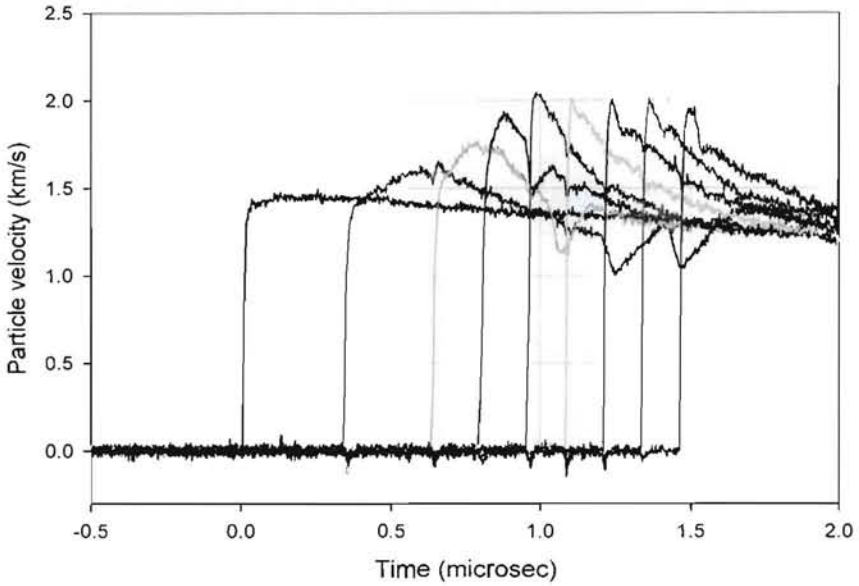

Figure 6. *In-situ* wave profiles showing the shock-to-detonation transition for shot 2S-361, 92.25/6.0/1.75 NM/1-4 mm silica/Guar, with an initial shock input pressure of 8.5 GPa

Over the range of shock input pressures sampled, the characteristics of the build-up to detonation were found to be similar. This type of behavior is indicated as "growth in and behind the front" in Table 1.

Interestingly, a range of initiation behaviors was observed as a function of the shock strength for gelled NM containing the 40 μm particles. At low pressures (< 6 GPa), reactive growth closely behind the shock front was observed, but the material did not turn-over to detonation within the time/distance of the gauge elements and 1-dimensionality of the experiment. At intermediate shock input pressures (7-8 GPa), some reactive growth was observed close to the front, followed by a the appearance and growth of a reactive wave behind the front, reminiscent of a superdetonation. This could be due to a thermal explosion behind the front, or a phase velocity associated with initiation from a point outside of the centerline behind the shock. This wave, traveling from behind, eventually overtakes the front, leading to an overdriven detonation. An example is shown in Fig. 7, for shot 2S-358, 92.25/6.0/1.75 NM/40 μm silica/Guar, with an initial shock input pressure of 7.8 GPa. Inspection of the wave profiles in Figure 7 reveal a drop in particle velocity in the gauge records associated with the Lagrangian positions ahead of the reactive wave, indicative of a possible thermal explosion similar to that observed in homogenous liquid explosives. This behavior is recorded in Table 1 as "mixed mechanism."

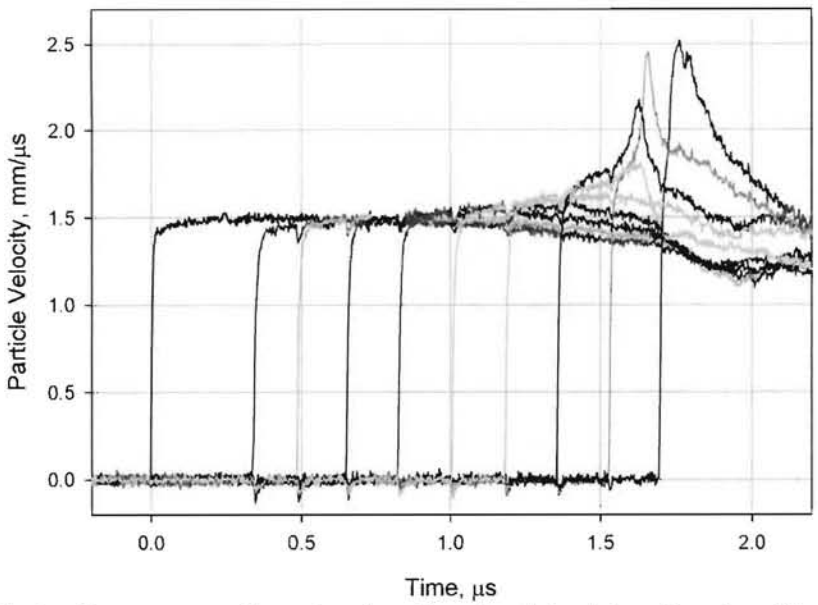

Figure 7. *In-situ* wave profiles showing the shock-to-detonation transition for shot 2S-358, 92.25/6.0/1.75 NM/40mm silica/Guar, with an initial shock input pressure of 7.8 GPa. (reprinted with permission, AIP)

At high shock input pressures (>9 GPa), homogeneous-like behavior, similar to that of neat NM, was observed with the transition to detonation occurring before any growth was observed near the shock front. This behavior is coincident with a "kink" or bending over of the data in the Pop-plot to parallel the data for neat NM. The wave profiles reveal the existence of a superdetonation wave traveling in the already-compressed material in all three experiments in this pressure regime, see, for example, Fig. 8. Inspection of the Pop-plot shows that the points for the heterogeneous-NM approach the Pop-plot for neat NM with a large slope, then bend over and parallel the neat NM data, coincident with the wave profiles reflecting a homogenous initiation mechanism for the three higher pressure points. So far, this behavior has been demonstrated at shock input pressures exceeding 9.5 GPa. This initiation mechanism is indicated as "homogeneous-like" in Table 1. To our knowledge, this is one of the few (if any) direct observations of a homogeneous initiation mechanism in a heterogeneous explosive formulation, and may be indicative of a limit in the critical hot spot size and/or temporal characteristics for interaction and growth during the timescales of the high shock input pressure regime for this mixture.

The insights gained from the embedded gauge measurements are consistent with Engelke's critical diameter work.[4-5] Here, we see that, *at high input shock pressures*, the silica beads appear to have little effect on the time to detonation (run distances) or reactive flow characteristics. From Engelke,[5] the beads are expected to be nominally 2 diameters apart. By increasing the number density and thus the distance between the particles, in the samples containing 6 wt% of 1-4 μm silica beads, the initiation behavior becomes more consistently "heterogeneous-like" at least over the input shock pressure regime sampled to date. Clearly, the nature of the shock-to-detonation transition is determined by the length and time scales associated with the confluence of hot spots formed from the shock wave interactions with the higher impedance particles in the mixtures, setting up a complex interplay between the innate chemical reactivity of the explosive, the shock strength, and hot spot evolution relative to the shock front. Here, we show in a simple system, that the reactive flow can be "tuned" through the variation of the number density and size of the particles, up to a limiting condition where the hot spots have no apparent influence on the initiation process.

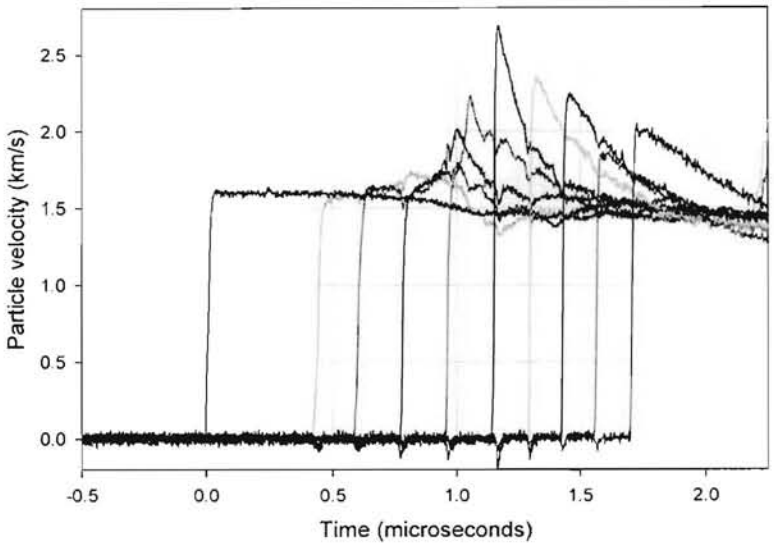

Figure 8. *In-situ* wave profiles showing the shock-to-detonation transition for shot 2S-317, 92.25/6.0/1.75 NM/40mm silica/Guar, with an initial shock input pressure of 9.5 GPa. (reprinted with permission, AIP)

Further examination of the wave profiles illustrates additional features of the detonation behavior of the mixtures. For the smaller silica beads, the *detonation* wave profiles show a "notch" in the wave near a particle velocity of $u_p \sim 1.8$ mm/μs. The notch is clearly visible in the profiles shown in Figure 6. This notch may be related to the kinetics associated with the chemical release of energy through the reaction zone, and the position of the sonic locus behind the front, or it may be related to the interaction of the detonation wave with the silica beads as they enter the flow field. Based on our recent measurements of the features of the chemical reaction zone for neat NM, and previous embedded gauge measurements on the neat liquid, it is also clear from the profiles that the von Neumann "spike" is being clipped by the temporal response function of the electromagnetic gauges (which is estimated to be ~ 10 ns). The peak particle velocity is lower than expected (for both neat NM and the mixtures studied here). Future work should include independent measurements of the chemical reaction zone associated with the steady detonation using VISAR (Velocity-Interferometer-System-for-Any-Reflector) or PDV (Photon Doppler Velocimetry). The detonation velocity for the mixture of 6 wt% 1-4 μm silica in gelled NM could also be estimated using the data from shot 2S-319. In this experiment, the turnover to detonation occurred near the impact interface, and the detonation appeared to be nearly-steady as recorded by the gauges located farther from the interface. The detonation velocity was found to be 6.152 ± 0.017 km/s from the response of one of the shock trackers, which compares well with the 6.167 ± 0.002 km/s reported for NM:silica by Engelke.[4]

SUMMARY AND CONCLUSIONS

We have examined the influence of shock impedance mismatches as a source of hot spots on the initiation characteristics of "heterogeneous"-NM. The reactive flow characteristics, and run distances-to-detonation for gelled NM with 6 wt% silica beads of two discrete sizes have been reported. The smaller beads, which are at a higher number density and closer interparticle spacing, were found to be more sensitizing than the larger beads. The results were seen as consistent with the failure characteristics observed for the same mixtures by Engelke. For the samples containing 6 wt% 40 μm beads in gelled nitromethane, a range of initiation behaviors

were observed for the first time. As the initial shock strength was varied, the behavior transitioned from "heterogeneous"-like, with growth in the front at low shock input pressures, to initiation via thermal explosion, and build-up of a reactive wave more characteristic of homogeneous explosives, at high pressures.

Future work will include additional variations of the size and number density of glass beads, and incorporation of hollow glass microballoons as a second type of hot spot. Measurements of the chemical reaction zone features will also add insights into the temporal attributes of the chemical energy release associated with detonation.

ACKNOWLEDGMENTS

Los Alamos National Laboratory is operated by LANS LLC for DOE and NNSA. Funding was provided by LANL Laboratory Directed Research and Development, Project #20080015DR. We gratefully acknowledge Ray Engelke for insightful discussions and the Chamber 9 gas gun team for help with the experiments.

REFERENCES

1. Bowden, F. P., Yoffe, A. D. *Initiation & growth of explosion in liquids and solids* (Cambridge, 1952).
2. Field, J. E. Acc. Chem. Res. 25, 489-496 (1992).
3. Bourne, N. K.; Field, J. E. *Proc.: Math., Phys., Eng. Sci.*, **455**, 2411 (1999).
4. Engelke, R. *Phys. Fluids*, **22**(9), 1623 (1979).
5. Engelke, R. *Phys. Fluids*, **26**(9), 2420 (1983).
6. Sheffield, S. A.; Dattelbaum, D. M. et al. in 13th International Sympsium on Detonation, Office of Naval Research, ONR 351-07-01, 401 (2006).
7. Ramsay, J. B.; Popolato, A. Fourth Symposium (International) on Detonation, Office of Naval Research Report # ACR-126, p 233 (1965).
8. Chick, M. C. Fourth Symposium (International) on Detonation, Office of Naval Research, ACR-126, 349-358 (1965).
9. Price, D. Fifth Symposium (International) on Detonation, Office of Naval Research, ACR-184, 207-217(1970).
10. Scott, C. L. Fifth Symposium (International) on Detonation, Office of Naval Research, ACR-184, 259-266 (1970).
11. Seely, L. B. Proceedings of the Fourth Elecric Initiator Symposium, Franklin Institute, PA, Paper 27 (1963).
12. Simpson, R. L.; Helm, F. H. et al. Ninth Symposium (International) on Detonation, OCNR-113291-7, 25-38 (1989).
13. Setchell, R. E. Eighth Symposium (International) on Detonation, NSWC MP 86-194, 15-25 (1985).
14. Moulard, H. Ninth Symposium (International) on Detonation, OCNR-113291-7, 18-24 (1989).
15. Moulard, H.; Kury, J. W.; Delclos, A. Eighth Symposium (International) on Detonation, NSWC MP 86-194, 902-913 (1985).
16. Lee, E. L.; Tarver, C. M. Phys. Fluids, 23, 2362-72 (1980).
17. Presles, H.-N. *et al.* Shock Waves, 4, 325-329 (1995).
18. Khasainov, B. A.; Ermolaev, B. S.; Presles, H.-N.; Vidal, P. Shock Waves, 7, 89-105 (1997).
19. Bouton, E. *et al.* Shock Waves, 9, 141-147 (1999).
20. Howe, P.; Frey, R.; Taylor, B.; Boyle, V. Sixth Symposium (International) on Detonation, Office of Naval Research, ACR-221, 11-19 (1976).
21. Sheffield, S. A.; Alcon, R. R. *Shock Compression of Condensed Matter-1989*, 683 (1990).

22. Gustavsen, R. L. ; Sheffield, S. A.; Alcon, R. R. "*High Pressure Science and Technology - 1993, Pts 1 and 2,* 1703-1706 (1994).
23. Alcon, R. R.; Sheffield, S. A.; Martinez, A. R.; Gustavsen, R. L.; *AIP Conference Proceedings* **429**, 845-848 (1998).
24. Bouyer, V.; Sheffield, S. A.; Dattelbaum, D. M.; Gustavsen, R. L.; Stahl, D. B.; Doucet, M.; Decaris, L. "Experimental Measurements of the Chemical Reaction Zone of Detonating Liquid Explosives;" AIP Conference Proceedings, 2009 accepted.
25. Engelke, R. *Phys. Fluids*, **23**(5), 875 (1980).
26. Campbell, A. W.; Davis, W. C.; Travis, J. R. *Phys. Fluids*, **4**, 511 (1961).
27. Chaiken, R. F. *J. Chem. Phys.*, **33**, 760 (1960).
28. Sheffield, S. A.; Engelke, R.; Alcon, R. R. in Ninth Symposium (International) on Detonation; 1989.
29. Hardesty, D.R.; Lysne, P. C. "Shock initiation and detonation properties of homogeneous explosives" Sandia Report no. SLA-74-165, 1974-05-01.
30. Voskoboinikov, I. M.; Bogomolov, V. M.; Apin, A. Ya. *Fizika Goreniya I Vzryva*, **4**, 45-49 (1968).
31. Leal, B. *et al.* In Proceedings of the 11th Symposium (International) on Detonation.
32. Engelke, R.; Sheffield, S. A.; Stacy, H. L. Phys. Fluids, 16, 4143 (2004).
33. Engelke, R.; Sheffield, S. A.; Stacy, H. L. Phys. Fluids, 17, 096102 (2005).
34. Cooper, P. W., Explosives Engineering (VCH, New York, 1996), p. 280.
35. Menikoff, R. personal communication, Los Alamos National Laboratory, November 2009.
36. Hill, L. G. *et al.* in *AIP Conference Proceedings*, Topical Group meeting on Shock Compression of Condensed Matter, 2009, *in press*.
37. Gustavsen, R. L.; Sheffield, S. A.; Alcon, R. R.; Hill, L. G.; "Shock Initiation of New and Aged PBX 9501 Measured with Embedded Electromagnetic Particle Velocity Gauges," Los Alamos National Laboratory Report, LA-13634-MS.